Long non-coding RNA LINC01960-201 hinders decidualization of endometrial stromal cell in endometriosis: Relevance to endometrial receptivity

HAN CAI[1,2] and JINGHE LANG[2]

[1]Department of Obstetrics and Gynecology, Beijing Chao-Yang Hospital, Capital Medical University, Beijing 100020; [2]Department of Obstetrics and Gynecology, Peking Union Medical College Hospital, Peking Union Medical College and Chinese Academy of Medical Sciences, Beijing 100730, P.R. China

Received May 5, 2020; Accepted September 20, 2021

DOI: 10.3892/mmr.2022.12883

Abstract. Emerging data have indicated that long non-coding RNAs (lncRNA) are associated with the pathogenesis of endometriosis. However, few are associated with endometriosis-associated infertility. In addition, to the best of our knowledge, the role of lncRNAs in decidual formation during the window of implantation with endometriosis has not been reported to date. Based on our previous results, the aim of the present study was to explore the role of lncRNA long intergenic non-protein coding RNA (LINC)01960-201 in *in vitro* decidualization of endometrial stromal cells in endometriosis during the window of implantation, as well as to explore the biological function of LINC01960-201, and the regulation of a disintegrin and metalloproteinase with thrombospondin motifs 7 (ADAMTS7), hsa-microRNA (miR)-760 and hsa-miR-608 in the decidualization of endometrial stromal cells with endometriosis. Using miRanda, PITA and RNAhybrid, the present study predicted which miRs share the common target gene ADAMTS7 with LINC01960-201 and the existence of regulatory targets. Dual luciferase vectors were constructed to extract the plasmids and measure the relative fluorescence values in order to estimate target regulatory association between LINC01960-201, ADAMTS7 and miRs. Mid-secretory endometrial tissues were collected from women with endometriosis-associated infertility. From these tissues, endometrial stromal cells were extracted and cultured as primary cultures. Medroxyprogesterone acetate (MPA) and 8-Bromoadenosine 3',5'-cyclic monophosphate (8-Br-cAMP) were added to induce *in vitro* decidualization, and to knockdown LINC01960-201 and transfect a hsa-miR-608 mimic at the same time. Reverse transcription-quantitative PCR and western blotting were conducted to compare the difference in gene expression between the experimental and negative control groups. No regulatory sites between LINC01960-201 and hsa-miR-608 were identified; however, potential regulatory sites were detected between hsa-miR-608 and the 3'-untranslated region (UTR) of ADAMTS7, whereas neither the 3'-UTR of LINC01960-201 or the 3'-UTR of ADAMTS7 had any regulatory targets with hsa-miR-760. During the process of decidualization of endometrial stromal cells by *in vitro* induction, the expression of hsa-miR-608 in the knockdown group was significantly higher compared with that of the negative control group after LINC01960-201-knockdown, and the expression of ADAMTS7 in the transfection group was significantly lower compared with that of the negative control group after hsa-miR-608 mimic transfection. In conclusion, it was hypothesized that LINC01960-201 played a notable regulatory role in the decidualization of endometrial stromal cells in women with endometriosis during the window of implantation, and its abnormal expression may lead to the decline of endometrial receptivity and recurrent abortions.

Correspondence to: Dr Jinghe Lang, Department of Obstetrics and Gynecology, Peking Union Medical College Hospital, Peking Union Medical College and Chinese Academy of Medical Sciences, 1 Shuaifuyuan, Dongcheng, Beijing 100730, P.R. China
E-mail: langjinghe1555@sina.com

Key words: endometriosis, endometrial receptivity, decidualization, long non-coding RNA LINC01960-201, a disintegrin and metalloproteinase with thrombospondin motifs 7

Introduction

Poor decidualization of endometrial stromal cells is an important cause for the decreased implantation rate of endometriosis (1). Implantation depends on endometrial receptivity and embryo quality (2,3), and the synchronization of both is needed for the guarantee of a successful pregnancy. This scrupulous biological process allows the embryo to complete the orientation, adhesion and penetration into the basal layer of epidermal cells and intrusion in the endometrial matrix (4). Decidualization refers to the differentiation of endometrial stromal cells into decidual cells with secretory function during the mid-secretory period of the normal menstrual cycle, which provides the basic conditions for embryo implantation and placental formation (5,6). It only occurs at the window of implantation, which is short and decisive. This usually occurs at days 20-24 of the normal menstrual cycle (7), 7-10 days after

ovulation, which is equivalent to the mid-secretory phase when the uterus accepts embryo implantation. Barragan *et al* (8) have reported that patients with endometriosis had significant amount of damage to the decidualization of eutopic endometrial stroma cells following *in vitro* induction compared with that of the control group. Decidual impairment is an important factor in endometriosis-associated sterility. Infertility resulting in endometriosis is due to morphological changes in the endometrium, hormonal disorders (9), immunity rejection (10) and abnormal state of gene expression (9,11,12).

Long non-coding RNAs (lncRNAs) are ncRNAs >200 nucleotides in length with extensive biological functions, such as regulation of growth and development. Similar to microRNAs (miRNAs/miRs) (13,14), lncRNAs play a role at the post-transcriptional level, and achieve biological action by regulating the transcriptional products of their target mRNA (15). Several studies have demonstrated that lncRNAs and miRNAs are closely associated with endometriosis-associated infertility (13,16-18). A previous study revealed that decreased expression of H19 in endometrial stromal cells in patients with endometriosis increases the biological activity of miRNA let-7, while inhibiting the expression of insulin-like growth factor-I (IGF-I) at the post-transcriptional level, thus reducing the proliferation of endometrial stromal cells. This indicated that H19-let-7-IGF-I signaling is likely to be a key element to the declined endometrial receptivity of endometriosis (13).

The exact mechanism responsible for infertility in endometriosis is still unknown, but its severity has endangered women's physical and mental health, and has influenced their quality of life, and even created a socio-economic burden. There are 4 million women suffering from different degrees of infertility in China (19), and 7 million worldwide (20), among which the major reason for infertility is endometriosis (20). A previous study has indicated that 25-50% of infertile patients have endometriosis, and 30-50% of patients with endometriosis have clinical symptoms of infertility (21). In order to improve women's overall fertility status, it is of great significance to explore the infertility of endometriosis. At present, there are few studies on the problems associated with the regulation of deficient decidualization with endometriosis. In particular, to the best of our knowledge, studies on the post-transcriptional regulation of decidualization of endometrial stromal cells have not been reported to date.

Based on our previous results (22), long intergenic non-protein coding RNA (LINC)01960-201 was selected as the target. According to bioinformatical analysis, it was demonstrated that hsa-miR-760 and hsa-miR-608 have a common target gene, ADAMTS7, with LINC01960-201. It was also confirmed by target point analysis that there is a target site between hsa-miR-608 and ADAMTS7. In the present study, clinical samples (endometrial tissues) were collected from five female patients with infertility due to endometriosis. Endometrial stroma cells were isolated for primary cell culture, and *in vitro* decidualization was induced. The present study aimed to explore the biological function of LINC01960-201, and the regulatory association between ADAMTS7, hsa-miR-760 and hsa-miR-608 in the decidualization of endometrial stromal cells with endometriosis in order to identify novel ways to solve problems caused by endometriosis, such as pelvic pain and infertility.

Materials and methods

Ethics statement. The present study was approved by the Ethics Committees of Peking Union Medical College Hospital and the Chinese Academy of Medical Sciences (Beijing, China; approval no. S-k332). Written informed consent was obtained from the five patients and all the specimens were acquired with the knowledge of the patients.

Bioinformatics analysis. The potential binding sites between LINC01960-201 and hsa-miR-760, LINC01960-201 and hsa-miR-608, ADAMTS7 and hsa-miR-760, ADAMTS7 and hsa-miR-608 were analyzed using miRanda (Memorial Sloan-Kettering; http://www.microrna.org/microrna/home.do), PITA (SegalLab; http://genie.weizmann.ac.il/pubs/mir07/mir07_dyn_data.html) and RNAhybrid (Behmsmeier; http://bibiserv.techfak.uni-bielefeld.de/rnahybrid/).

Vector construction and plasmid extraction. DNAMAN software 8.0 (Lynnon Biosoft) analyses of the 3'-untranslated region (UTR) sequences and vector (pmiR-RB-REPORT™ dual luciferase reporter vector) of the target genes LINC01960-201 and ADAMTS7 were performed. Primer design was based on the base pairing principle (Table I), and 293T cell genomic DNA was used as the template. The 3'-UTR fragments of LINC01960-201 and ADAMTS7 were amplified using PCR. The PCR products were subjected to 1.5% agarose gel electrophoresis and then purified. Two restriction enzymes, *Xho*I and *Not*I, were used for digesting the target gene segment and vector, respectively. The target gene fragment was cloned into the vector using PCR. The junction products were transformed into DH5α receptive cells (Tiangen Biotech Co., Ltd.), amplicillin-containing antibiotic Luria-Bertani (LB) broth (Tinagen Biotech Co., Ltd.) was added (antibiotic concentration, 100 μg/ml), and five colonies were selected for PCR. The products were examined using 1.5% agarose electrophoresis, and the positive clones were further identified by sanger sequencing (23). Next, the colonies were expanded and cultured to extract the plasmid. The sequencing results of the recombinant plasmid were evaluated using the SnapGene® Viewer 2.8.3 (from GSL Biotech; available at snapgene.com) through Basic Local Alignment Search Tool comparison (Genbank; NM_014272.4) (Figs. S1 and S2). The properly sequenced bacterial liquid was transferred to 10 ml LB liquid medium containing the corresponding antibiotics and cultured overnight at 37˚C. Plasmid extraction was carried out with the TIANprep Mini Plasmid kit (Tiangen Biotech Co., Ltd.) according to the manufacturer's instructions.

Dual luciferase reporting experiment. According to the manufacturer's instructions, miRNA mimics or non-targeting control (24,25) (hsa-miR-608 mimic sequence: 5'-AGGGGUGGUGUUGGGACAGCUCCG UUCCCCACCACAACCCUGUCGAGGCA-3'; Guangzhou RiboBio Co., Ltd.), target gene 3'-UTR dual reporter vector or mutant vector plasmid (Guangzhou RiboBio Co., Ltd.) and Lipofectamine™ 3000 reagent (Invitrogen; Thermo Fisher Scientific, Inc.) were mixed and transfected into A549 cells, cells were plated in 96-well plates at a density of $1.5x10^4$ cells/ml at 37˚C. All reactions were performed

Table I. Primer sequence used to construct a luciferase vector containing the target gene 3' untranslated region.

Primer name	Sequence (5'-3')	Length (bp)
h-LINC01960-201-F-(1) (XhoI)	CGG(CTCGAG)CTCTGGTCTCCTGACTCTGG	1
h-LINC01960-201-R-(1884) (NotI)	AAT(GCGGCCGC)TTATATTTCACCCTTAAATACTTT	1,884
h-LINC01960-201-MUT2 (278)	GCCTTGTC(GGGTGGGC)CTTGGCTCGCGTTCTGAA	278
h-LINC01960-201-MUT2 (304)	GAGCCAAG(GCCCACCC)GACAAGGCTCCTCCGGGG	304
h-LINC01960-201-MUT1 (754)	CTCCGCAG(GGTCCCGG)CAGGAGGCCGCTCTTCCG	754
h-LINC01960-201-MUT1 (780)	GCCTCCTG(CCGGGACC)CTGCGGAGGCGACAGGCT	780
h-ADAMTS7-3UTR-F-(1) (XhoI)	CGG (CTCGAG) CTGCGCCAGGATGCACAGA	1
h-ADAMTS7-3UTR-R-(218) (NotI)	AAT(GCGGCCGC)TGCTTTGGAATGGTAGATGCT	218
h-ADAMTS7-3UTR-MUT1-F (27)	ACAGACCT(GTCACGG)CACCACGGGCTGTGGCGG	27
h-ADAMTS7-3UTR-MUT1-R (52)	CCGTGGTG(CCGTGAC)AGGTCTGTCGGTCGGTCT	52
h-ADAMTS7-3UTR-MUT2-F (59)	GGAGCTCC(GCGGGG)CTGCGCCCTAATGGTGCT	59
h-ADAMTS7-3UTR-MUT2-R (81)	GGGCGCAG(CCCCGC)GGAGCTCCGCCACAGCCC	81

Parentheses in the sequence indicates XhoI and NotI restriction sites; LINC, long intergenic non-protein coding RNA.

in triplicate. At 48 h post-transfection, Dual-Glo® Stop & Glo buffer (Promega Corporation) was added to start the Dual-Glo Luciferase Assay System (Promega Corporation) and a luminometer (Veritas 9100-002; Promega Corporation) was used to measure the fluorescence value. The reported fluorescence of the vector was *Renilla* luciferase (hRluc), and the corrected fluorescence was luciferase (hluc). The 3'-UTR region of the gene was cloned downstream of the hRluc gene. Since miRNAs act on the target gene through the 3'-UTR region, miRNAs were co-transformed with the constructed reporter vector, and the interaction between miRNA and target gene was verified by the decrease in the relative fluorescence value of the reporter gene.

Patients and samples. From June to September 2017, the endometrial tissues of female patients mainly affected by 'infertility due to endometriosis' who underwent hysteroscopy and laparoscopy at Peking Union Medical College Hospital (Beijing, China) were collected. Their mean age was 30±2.9 years. All patients underwent laparoscopic excision of ovarian endometriomas and hysteroscopy examination at mid-secretion time (19-24 days of the normal menstrual cycle). According to the revised American Fertility Society (American Society of Reproductive Medicine Staging, as amended in 1997), all the patients were clinical stage III-IV (26). The exclusion criteria included other endocrine diseases such as diseases of the adrenal and pituitary glands, uterine fibroids and genital tuberculosis. None of the patients had been treated with hormonal drugs for ~3 months. The patients were diagnosed with endometriosis by laparoscopy and verified by clinical pathology. All the tissues were collected under sterile conditions, washed with physiological saline and placed into aseptic freezers without enzymes at -20˚C. The primary cells were extracted for culture on the day of dry ice transportation.

Primary cell culture and in vitro induction of decidualization. Endometrial tissue was placed in a cell culture dish with its 2-3 times volume (ml) of DMEM/F12 phenol red-free medium (HyClone; Cytiva), cut into pieces of 0.5-1.0 mm with ophthalmic scissors until visually mushy and then placed in a 15-ml centrifuge tube with the appropriate quantity of medium. Next, 0.1% collagenase I (Gibco; Thermo Fisher Scientific, Inc.) was added and digested at 37˚C for 1 h. After filtering through a 150-μm 100-mesh cell strainer, the filtered endometrial stromal cells were immediately centrifuged at 1,000 x g for 5 min at room temperature. Next, 2 ml 0.25% trypsin (Gibco; Thermo Fisher Scientific, Inc.) was added, and the cells were digested for 10 min. The reaction was terminated by adding 2 ml dextran charcoal stripped-fetal bovine serum (DCC-FBS; HyClone; Cytiva). Upon centrifugation at 1,000 x g for 5 min at room temperature, the supernatant was discarded and the pellet was added to a 25-mm culture bottle. Next, an appropriate quantity of DMEM/F12 phenol red-free medium (HyClone; Cytiva) with 10% DCC-FBS and 1% penicillin-streptomycin was added, and the cells were cultured at 37˚C in a 5% CO_2 incubator (Thermo Fisher Scientific, Inc.). After 24 h, the adherent cells were observed under an optical microscope (magnification, x40), while the non-adherent cells and the blood cells were discarded. The cells were replaced with DMEM/F12 phenol red-free medium (HyClone; Cytiva), which was then replaced every 2-3 days. Microscopic observation (Nikon Corporation) revealed that the cells were overgrown in culture vials, and were subcultured by using 0.25% trypsin at a 1:2 ratio for 3-4 generations. Phenol red-free DMEM/F12 with 2% DCC-FBS, 0.5 mmol/l 8-Bromoadenosine 3',5'-cyclic monophosphate (8-Br-cAMP; Sigma-Aldrich; Merck KGaA) and 1 μmol/l medroxyprogesterone acetate (MPA; Sigma-Aldrich; Merck KGaA) were added to induce decidualization *in vitro*, and for concomitant knockdown and transfection.

LINC01960-201-knockdown and hsa-miR-608 mimic transfection. siRNA and miRNA mimic sequences are presented in Table II. Endometrial stroma cells were digested with trypsin, and DMEM/F12 phenol red-free medium (HyClone; Cytiva) was added. Cells at a density of $2x10^5$ cells were cultured in

Table II. Sequences of LINC01960-201 silencer and hsa-miR-608 mimic.

Gene	Target sequence (5'-3')
Ribo™ h-LINC01960-201 Smart Silencer	ATTCCTCCCAACAGCTGGAT GCTTAAGAGGGTCAACGTGT TCCAGACCTTAGTCACTCTG TGCACAACCTCAGGAAACA AGACCTTAGTCACTCTGCT CACGTAACAACCAAATGCA
hsa-miR-608 mimic	AGGGGUGGUGUUGGGAC AGCUCC GUUCCCCACCACAACCCU GUCGAGGCA

Table III. Primers for reverse transcription-quantitative PCR.

Primer name	Sequence (5'-3')
lncDETECT™ h-LINC01960_ qPCR_1085 bp	F: CTATTGCACAACCTCAGGAAACAG R: TGGGAAAGGAAAACACACTTCA
GAPDH	F: GAACGGGAAGCTCACTGG R: GCCTGCTTCACCACCTTCT
U6	F: CTCGCTTCGGCAGCACA R: AACGCTTCACGAATTTGCGT

F, forward; R, reverse.

a 24-well plate. In total, three replicates of each sample and three negative controls (NCs) were prepared. Briefly, Ribo™ lncRNA Smart Silencer (Guangzhou RiboBio Co., Ltd.) or the NC siN0000001-1-5 siR NC #1 (Guangzhou RiboBio Co., Ltd.) was added to a 24-well plate at a concentration of 100 nM, and riboFECT™ CP reagent (Guangzhou RiboBio Co., Ltd.) was added. After being lightly agitated until thoroughly mixed, the samples were incubated at room temperature for 15 min. Next, an appropriate quantity of medium was added to the mixture and shaken gently until fully mixed. Subsequently, 1 μmol/l MPA and 0.5 mmol/l 8-Br-cAMP were added to induce the decidualization of endometrial cells *in vitro*, and the well-mixed 24-well plate was placed into a CO_2 cell incubator at 37˚C for 48 h. The differential expression levels of hsa-miR-608 between the LINC01960-201-knockdown groups and the negative controls, as measured using reverse transcription-quantitative PCR (RT-qPCR), were used to evaluate the effect of lncRNA-knockdown on the expression of hsa-miR-608 in the positive control group, in order to explore the mutual regulation between LINC01960-201 and hsa-miR-608.

Next, hsa-miR-608 mimic (Guangzhou RiboBio Co., Ltd.) or the NC miR1N0000001-1-5 micrON mimic NC #22 (Guangzhou RiboBio Co., Ltd.) was added to a 24-well plate at a concentration of 50 nM, followed by addition of riboFECT™ CP reagent (Guangzhou RiboBio Co., Ltd.). After being lightly shaken until thoroughly mixed, the mixture was incubated at room temperature for 15 min. Next, an appropriate quantity of medium (464.5 μl) was added to the mixture and shaken gently until fully mixed. Subsequently, 1 μmol/l MPA and 0.5 mmol/l 8-Br-cAMP were added to induce the decidualization of endometrial cells *in vitro* and the well-mixed 24-well plate was placed into a CO_2 cell incubator at 37˚C for 48 h. Western blotting was used to detect the expression of ADAMTS7 after hsa-miR-608 mimics transfection.

RT-qPCR. According to the manufacturer's protocol, TRIzol (Invitrogen; Thermo Fisher Scientific, Inc.) was used to extract the total RNA from the decidual cells. The primers used in the present study are presented in Table III. For miRNA quantification, Bulge-loop™ miRNA qRT-PCR Primer Sets (one RT primer and a pair of qPCR primers for each set) specific for hsa-miR-608 were designed by Guangzhou RiboBio Co., Ltd. (cat. no. MQPS0001954-1-100). The FastQuant RT kit (Tiangen Biotech Co., Ltd.) was used for the RT of total RNA. Total RNA (1 μg) and 20 μl reaction system (10X Fast-RT Buffer, 2 μl; FQ-RT Primer Mix, 2 μl; RT Enzyme Mix, 1 μl; RNase-free water, 5 μl; and buffer, 10 μl) were subjected to 42˚C for 15 min and 95˚C for 3 min, followed by cooling on ice and RT. The same quantity of RNA was used for all samples. The qPCR reaction system (10 μl) consisted of 5 μl 2X Power SYBR® Green PCR Master Mix (Applied Biosystems; Thermo Fisher Scientific, Inc.), 0.5 μl complementary DNA sample, 0.25 μl forward primer (10 μM), 0.25 μl reverse primer (10 μM) and 4 μl nuclease-free water. A MicroAmp Optical 96-well reaction plate (Applied Biosystems; Thermo Fisher Scientific, Inc.) was used. Denaturation was carried out at 95˚C for 10 min in a QuantStudio™ 7 Flex Real-Time PCR system (Applied Biosystems; Thermo Fisher Scientific, Inc.). Next, 40 cycles of 95˚C for 15 sec and 60˚C for 1 min, and a final extension at 60˚C for 10 min were performed, before subjecting the samples to 95˚C for melting curve analysis (temperature ramp of 2%). All reactions were performed in triplicate. Electrophoresis (2.0% agarose gel) was used to detect the amplification specificity of the products. U6 was selected as the internal reference gene. Expression was measured using the $2^{-\Delta\Delta Cq}$ method (27).

Protein extraction and western blotting. The decidualized endometrial cells were washed two to three times with PBS. Next, 250 μl RIPA lysis buffer (containing freshly added protease inhibitors) was added to the plate for 3-5 min. The culture plate was shaken repeatedly to allow the reagent to be in full contact with the cells. Next, cells and reagents were scraped off with a cell scraper and collected into a 1.5-ml centrifuge tube and cooled on ice for 30 min. Repeated blowing with a pipette ensured that the cells were completely lysed. After centrifugation at 13,000 x g for 10 min at 4˚C, the supernatant was kept and a bicinchoninic acid kit (Wuhan Servicebio Technology, Co., Ltd.) was used to determine the protein concentration. The protein solution [mixed at a 4:1 ratio with 5X protein sample buffer (Wuhan Servicebio Technology, Co., Ltd.)] was boiled for 15 min and stored at -20˚C until use. Proteins (30 μg per lane) were separated using 10% SDS-PAGE and then transferred to polyvinylidene difluoride

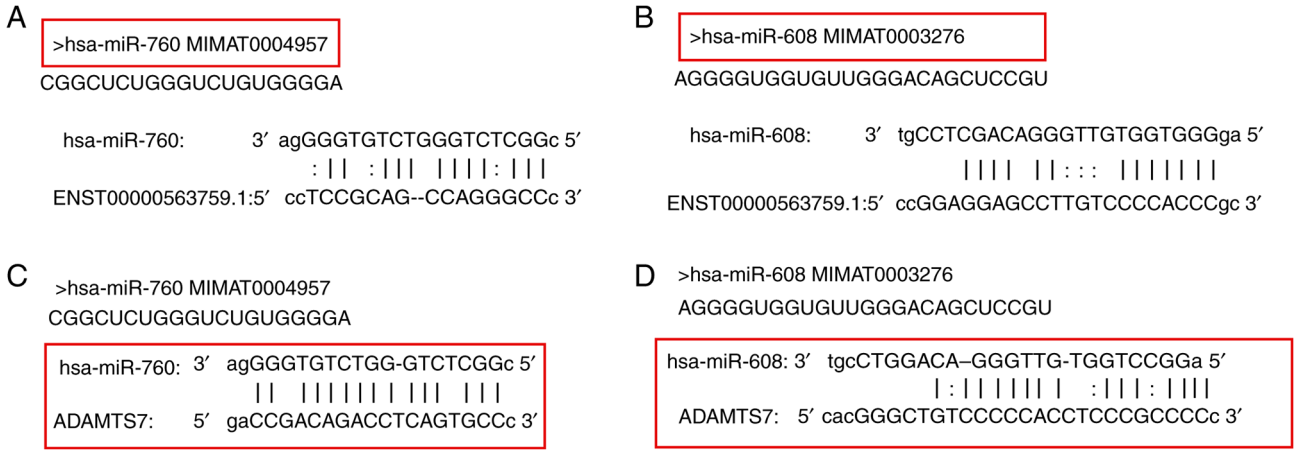

Figure 1. Graphic algorithms describing the binding sites of hsa-miR-760 and hsa-miR-608 predicted using miRanda, PITA and RNAhybrid. Binging sites between (A) LINC01960-201 and hsa-miR-760, (B) LINC01960-201 and hsa-miR-608, (C) ADAMTS7 and hsa-miR-760 and (D) ADAMTS7 and hsa-miR-608. miR, microRNA; ADAMTS7, a disintegrin and metalloproteinase with thrombospondin motifs 7; LINC, long intergenic non-protein coding RNA.

membranes, which were blocked with 5% skimmed milk for 1 h at room temperature. Next, the membranes were incubated with primary antibodies against ADAMTS7 (1:1,000; cat. no. 250456; Abbiotec, Inc.) at 4˚C overnight, followed by washing with TBS containing 0.05% Tween-20 (TBST) three times at room temperature. Next, the secondary antibody HRP-labeled goat anti-rabbit (1:3,000; cat. no. GB23303; Wuhan Servicebio Technology, Co., Ltd.) was added and incubated at room temperature for 30 min. The membranes were then washed in TBST, and detection by chemiluminescence (ECLA and ECLB; cat. no. G2014; Wuhan Servicebio Technology, Co., Ltd.) was carried out. Adobe Photoshop CS5 (Adobe Systems, Inc.) was used for image analysis. β-actin (1:3,000; cat. no. GB12001; Wuhan Servicebio Technology, Co., Ltd.) was selected as an internal reference. Grey value analysis (alphaEaseFC4.0; ProteinSimple) was conducted.

Statistical analysis. SPSS 19.0 (IBM Corp.) was used for data processing and statistical analysis. All RT-qPCR reactions were performed in triplicate. All data are expressed as the mean ± standard deviation and were analyzed using ANOVA with post hoc Tukey's test. $P<0.05$ was considered to indicate a statistically significant difference.

Results

Bioinformatics analysis. The potential target sites between LINC01960-201 and hsa-miR-760, LINC01960-201 and hsa-miR-608, ADAMTS7 and hsa-miR-760 and ADAMTS7 and hsa-miR-608 were predicted using bioinformatical analysis of the data using miRanda, PITA and RNAhybrid. Binding sites were identified in the 3'-UTR of LINC01960-201 and ADAMTS7. The predicted binding sites are presented in Fig. 1A-D. The potential target sites were analyzed by bioinformatics.

PCR amplification of the target gene. The primer length of LINC01960-201 was 1,884 bp, and the PCR product of lncRNA sequencing was consistent with the size of the LINC01960-201 band. A DNA band was generated at ~1.884 bp (Fig. 2A) that was approximately the expected size, indicating that the 3'-UTR of the LINC01960-201 gene was successfully amplified.

The target fragment of ADAMTS7 was amplified, and the amplified product was subjected to agarose gel electrophoresis. A single band was observed at ~218 bp (Fig. 2B), and the size was uniform with the target gene ADAMTS7. Overall, PCR amplification of the target gene was successful.

PCR and enzymatic digestion-mediated identification of the recombinant plasmid. As one of the primers was located in the target gene and the other one was located in the vector, it was verified that the vector plasmid was successfully linked to the target gene. The emolic electrophoretic bands illustrated that a splicing reaction in the constructed LINC01960-201 plasmid produced DNA bands at ~2,000 bp (Fig. 3A) and 400 bp (Fig. 3B) at ADAMTS7, which are the sizes of the expected fragments. Overall, the recombinant vector plasmid was successfully linked to the target gene.

Plasmid sequencing results. The 3'-UTR of LINC01960-201 sites 1 (CCAGGGCC muted to GGTCCCGG) and sites 2 (CCCACCCG muted to GGGTGGGC) (Figs. 4 and 5) and the 3'-UTR of ADAMTS7 sites 1 (CAGTGCC muted to GTCACGG) and sites 2 (CGCCCC muted to GCGGGG) (Figs. 6 and 7) were successfully mutated. Overall, the mutation of 3'-UTR of LINC01960-201 and the 3'-UTR of ADAMTS7 was successful. Following sequencing of the recombinant plasmid LINC01960-201, the following SNP was detected: C/G at 539 bp on NCBI (SNP number: rs11693010; https://www.ncbi.nlm.nih.gov/snp/). In addition, the A was mutated to C at 422 bp (the non-SNP site) (Fig. S1). Following sequencing of the recombinant plasmid ADAMTS7, the following SNP was detectedt: C/T at 42 bp on NCBI (SNP number: rs1045130) (Fig. S2).

Results of relative luciferase activity detection. In the present study, There was no significant difference in the double luciferase activity of human-LINC01960-201-WT and hsa-miR-760 co-transfected with the NC group. There was

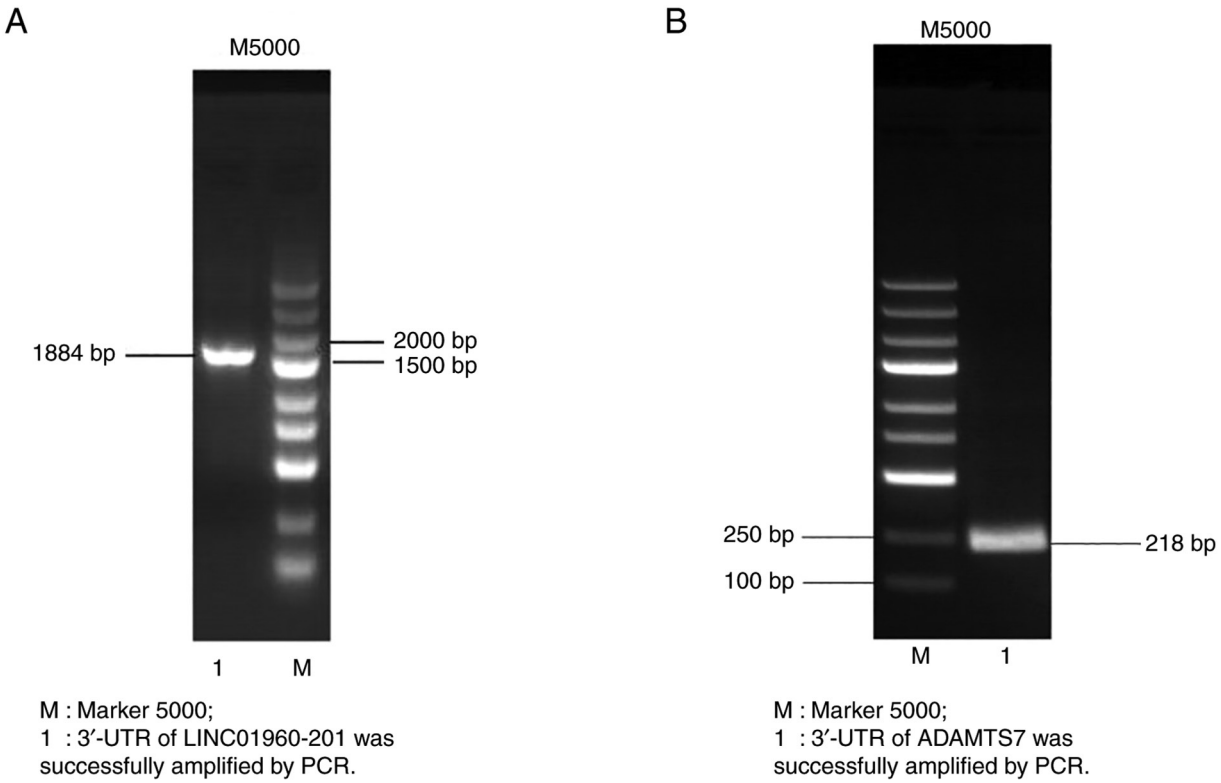

Figure 2. Agarose electrophoresis analysis of the PCR product of target genes in the 3' untranslated region, M5000. Amplification size is consistent with the theoretical size of (A) long intergenic non-protein coding RNA 01960-201 and (B) a disintegrin and metalloproteinase with thrombospondin motifs 7.

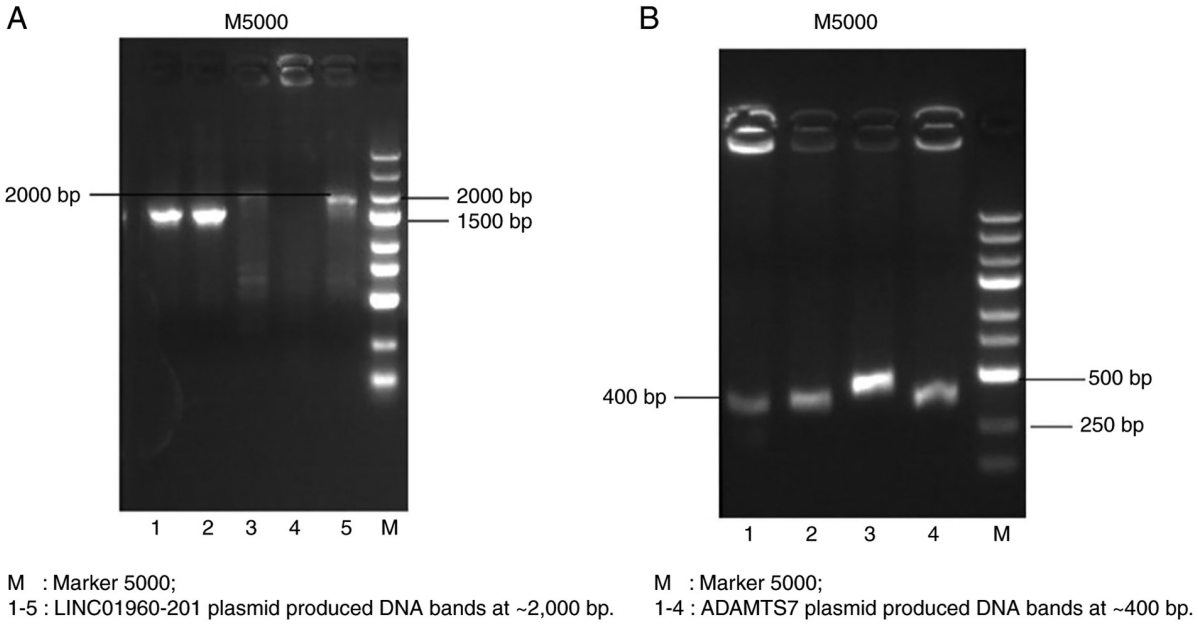

Figure 3. Agarose electrophoresis analysis of the PCR product of the PCR product of target genes in the 3' untranslated region, M5000. Size of bacteria P is consistent with the theoretical sizes of (A) long intergenic non-protein coding RNA 01960-201 and (B) a disintegrin and metalloproteinase with thrombospondin motifs 7.

no significant difference in the double luciferase activity of LINC01960-201-MUT1 and hsa-miR-760 co-transfected with the NC group (Fig. 8A).

The double luciferase activity of human-LINC01960-201-WT co-transfected with hsa-miR-608 was not significantly different from that of the NC group. There was no significant difference in the double luciferase activity of the LINC01960-201-MUT2 and hsa-miR-608 co-transfected with the NC group. These results indicated that hsa-miR-760 and hsa-miR-608 had no significant interaction with this segment of the 3'-UTR side of human-LINC01960-201 (Fig. 8B).

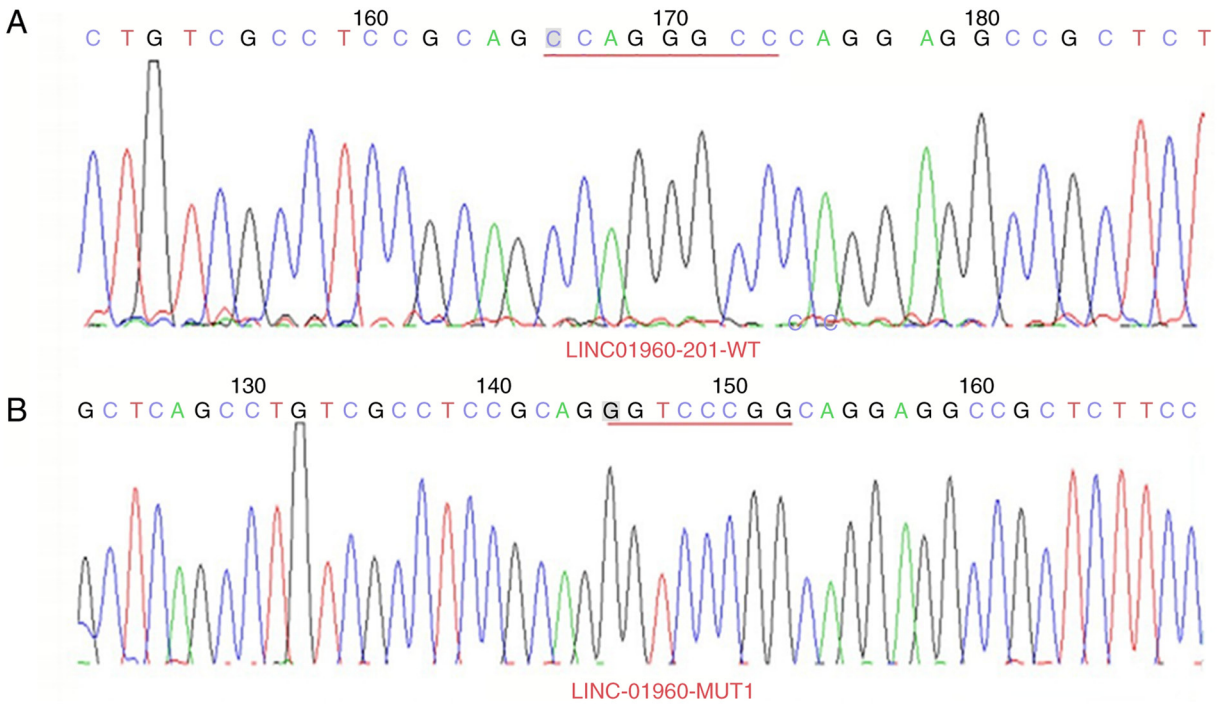

Figure 4. Site one (LINC01960-201):CCAGGGCC (763-770) were mutated into GGTCCCGG. (A) Partial sequencing peak of WT LINC01960-201 in 3'-UTR. (B) Sequencing peak map of MUT type 1 of LINC01960-201 in the 3'-UTR. UTR, untranslated region; WT, wild-type; MUT, mutant; LINC, long intergenic non-protein coding RNA.

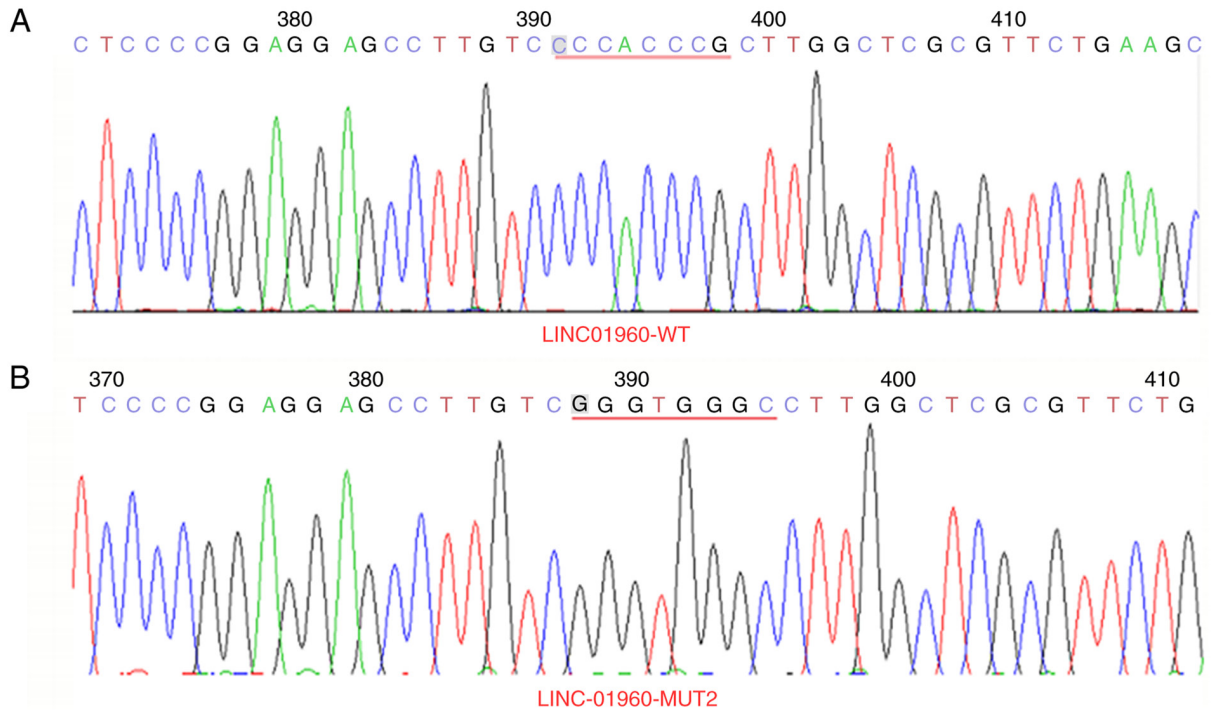

Figure 5. Site two (LINC01960-201):CCCACCCG (287-294) were mutated into GGGTGGGC. (A) Partial sequencing peak of WT LINC01960-201 in the 3'-UTR. (B) Sequencing peak map of MUT type 2 of LINC01960-201 in 3'-UTR. UTR, untranslated region; WT, wild-type; MUT, mutant; LINC, long intergenic non-protein coding RNA.

The hsa-miR-760 mimic had no significant effect on the reported fluorescence expression of human-ADAMTS7-WT or human-ADAMTS7-MUT1. There was no significant difference in the double luciferase activity of human-ADAMTS7-WT co-transfected with hsa-miR-760 compared with the NC group, and there was no significant difference in the double luciferase activity of human-ADAMTS7-MUT1 co-transfected with hsa-miR-760 compared with the NC group. The results indicated that hsa-miR-760 mimic had no significant interaction with the 3'-UTR of the human-ADAMTS7 gene (Fig. 8C).

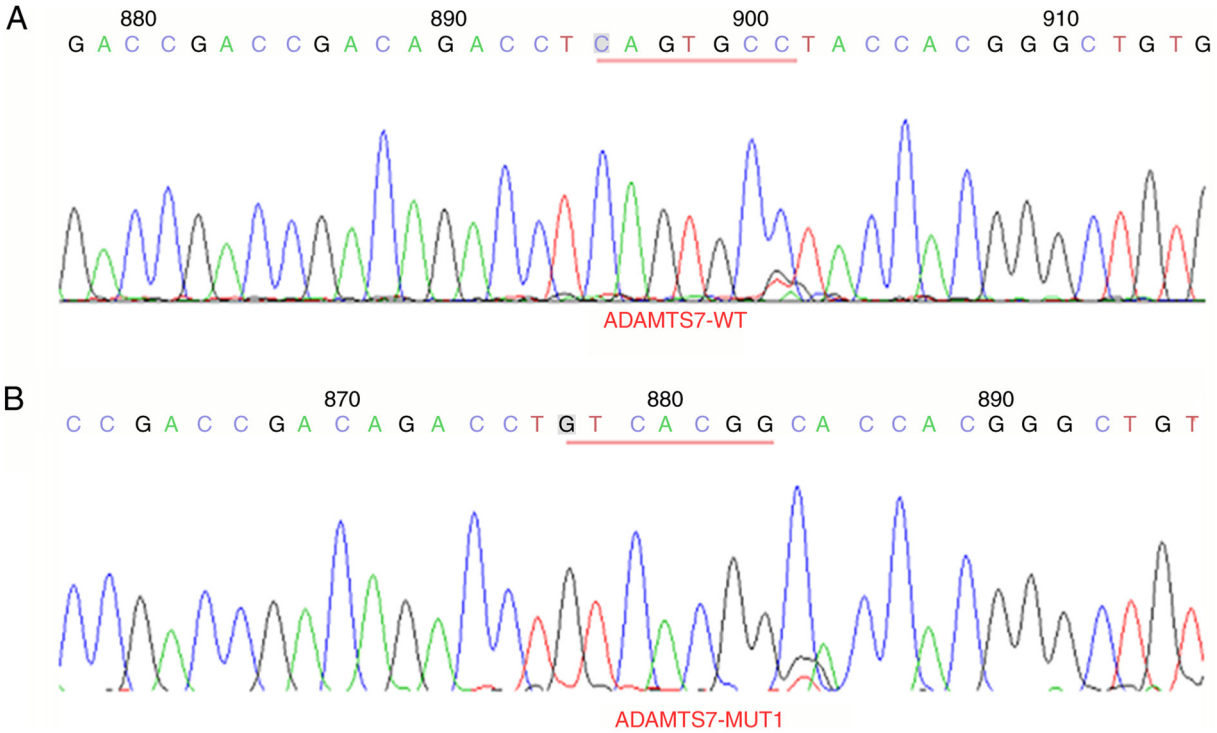

Figure 6. Site one (ADAMTS7):CAGTGCC were mutated into GTCACGG. (A) Partial sequencing peak of WT ADAMTS7 in 3'-UTR. (B) Sequencing peak map of MUT type 1 of ADAMTS7 in the 3'-UTR. UTR, untranslated region; WT, wild-type; MUT, mutant; ADAMTS7, a disintegrin and metalloproteinase with thrombospondin motifs 7.

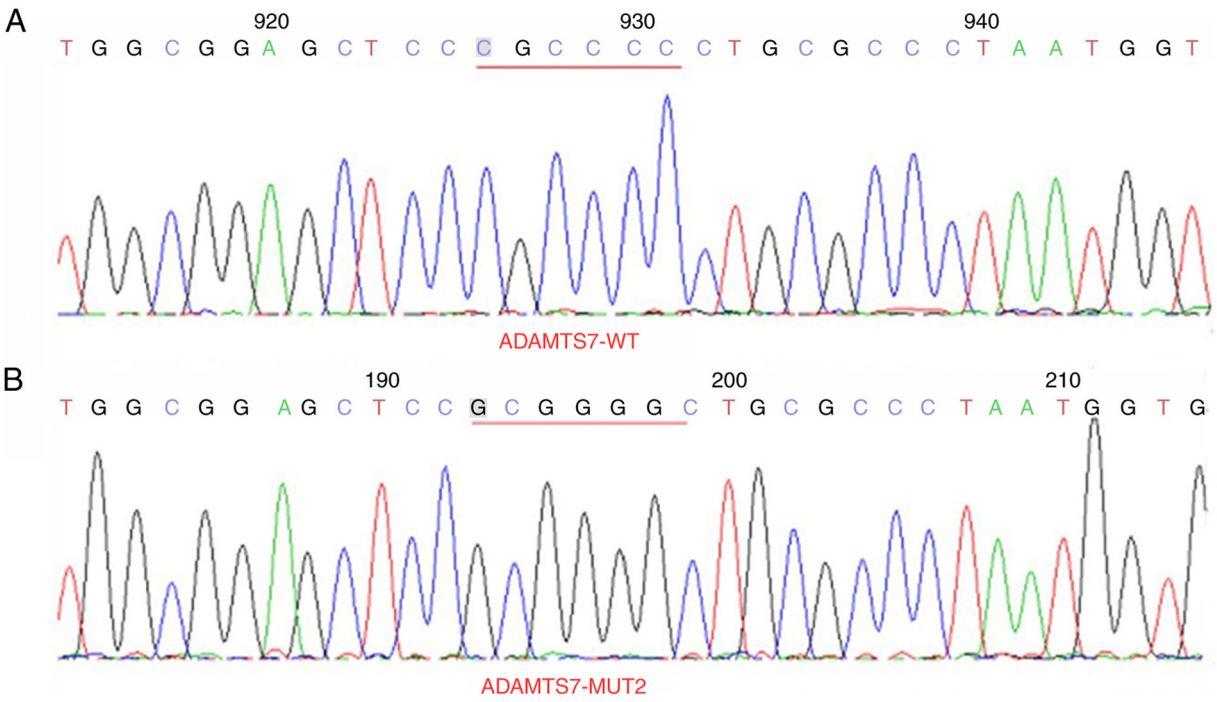

Figure 7. Site two (ADAMTS7):CGCCCC were mutated into GCGGGG. (A) Partial sequencing peak of WT ADAMTS7 in the 3'-UTR. (B) Sequencing peak map of MUT type 2 of ADAMTS7 in the 3'-UTR. UTR, untranslated region; WT, wild-type; MUT, mutant; ADAMTS7, a disintegrin and metalloproteinase with thrombospondin motifs 7.

The double luciferase activity of human-ADAMTS7-WT co-transfected with hsa-miR-608 was significantly lower than that of the NC group, while the double luciferase activity of human-ADAMTS7-MUT2 co-transfected with hsa-miR-608 was not significantly different from that of the NC group. Compared with that of the NC, hsa-miR-608 mimic had a more pronounced downward effect on human-ADAMTS7-WT report fluoridation. After mutating

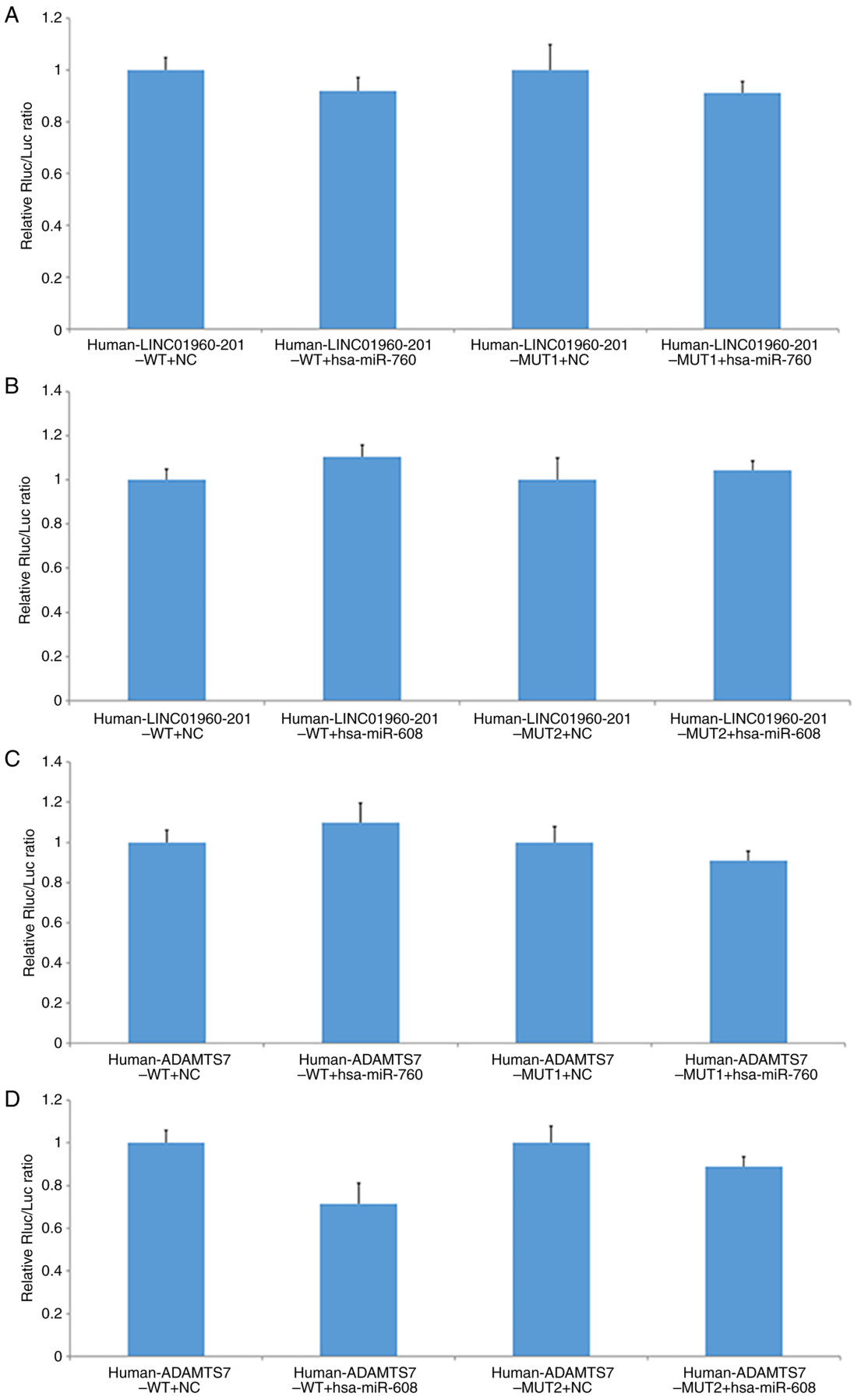

Figure 8. Relative fluorescence activity in each group of cells. Measurements of the relative relationship between (A) LINC01960-201 and hsa-miR-760, (B) LINC01960-201 and hsa-miR-608, (C) ADAMTS7 and hsa-miR-760 and (D) ADAMTS7 and hsa-miR-608. miR, microRNA; ADAMTS7, a disintegrin and metalloproteinase with thrombospondin motifs 7; MUT, mutant; WT, wild-type; NC, negative control; Rluc, *Renilla* luciferase; Luc, luciferase; LINC, long intergenic non-protein coding RNA.

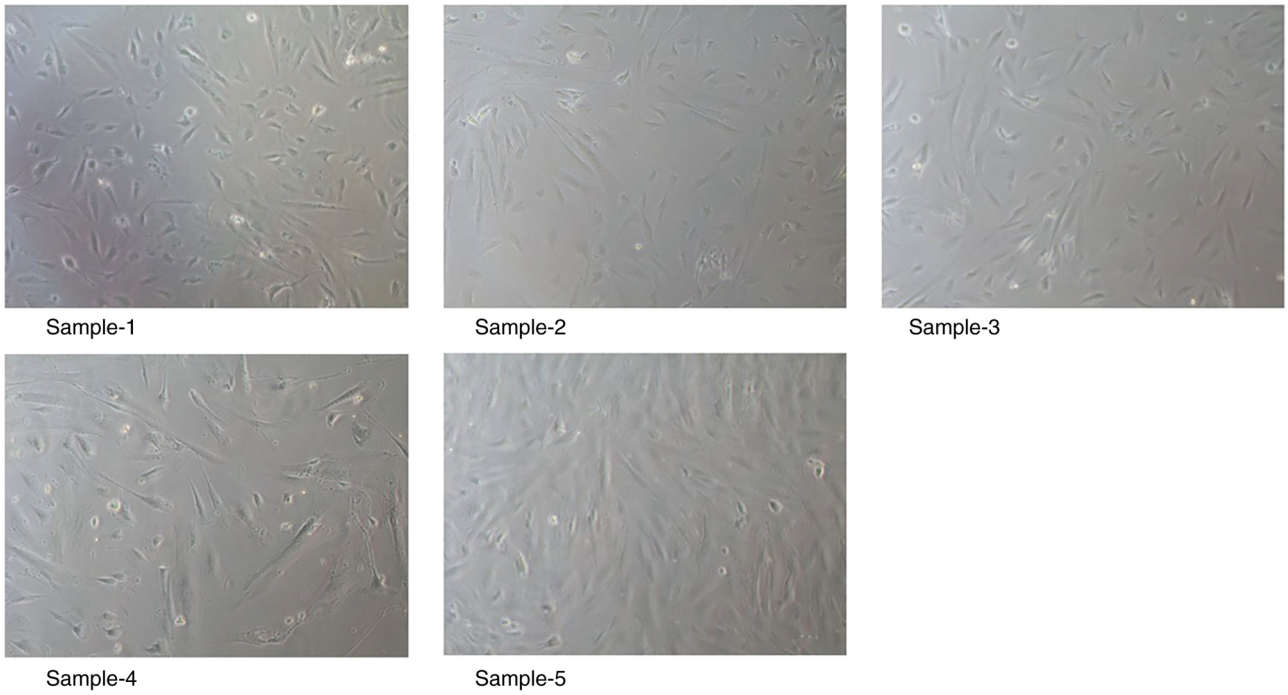

Figure 9. Morphology of primary endometrial stromal cells under light microscope. The samples come from each of the patients. Magnification, x400.

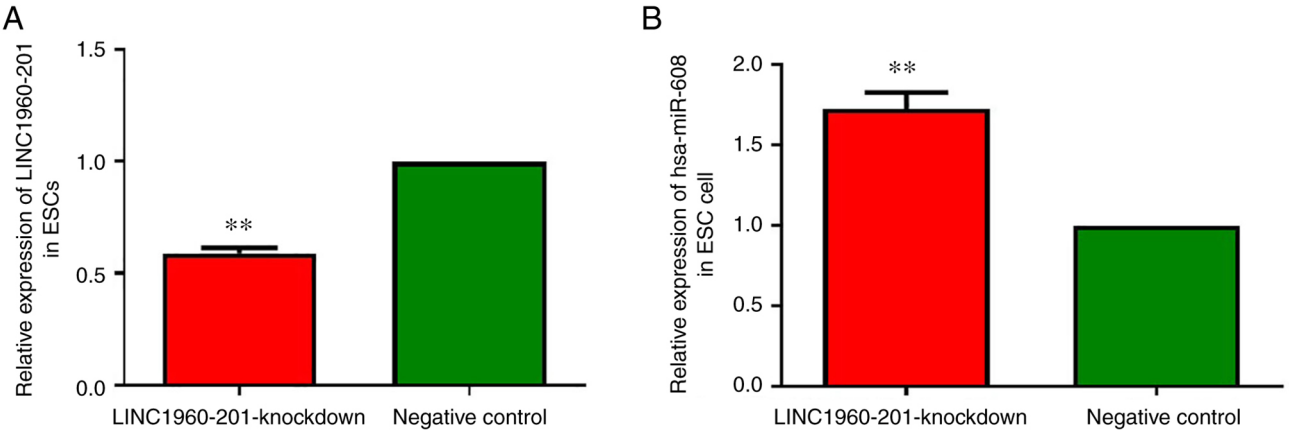

Figure 10. Expression of hsa-miR-608 is upregulated after transfection of si-LINC01960-201. (A) Changes in the expression of the LINC01960-201 between the two groups after LINC01960-201-knockdown. (B) Changes in the relative expression of hsa-miR-608 between the two groups after LINC01960-201-knockdown. **P<0.01 vs. the negative control. miR, microRNA; ESCs, endometrial stromal cells; LINC, long intergenic non-protein coding RNA.

its predicted target point, the reported fluorescence in the mutant vector human-ADAMTS7-MUT2 was restored. These results suggested that hsa-miR-608 mimic may regulate the expression of the gene through this site on the 3'-UTR of human-ADAMTS7 (Fig. 8D). Overall, there was evidence of significant regulatory sites between the 3'-UTR of ADAMTS7 and hsa-miR-608.

Primary culture of endometrial stromal cells in endometriosis. A total of five samples of eutopic endometrial tissues in women with endometriosis were collected, and the success rate of endometrial stromal cell isolation and culture was 100%. Adherent proliferation of the cells was observed a common optical microscope, which revealed a triangular shuttle shape of the cells with the cell nucleus circular centered. There was no significant difference in cell morphology between each group. The results of cell culture are presented in Fig. 9. Overall, primary culture of endometrial stromal cells in endometriosis was successful.

Changes in gene expression of after LINC01960-201-knockdown. The expression of LINC01960-201 was decreased during decidualization induced by 1 μmol/l MPA and 0.5 mmol/l 8-Br-cAMP in endometrial stromal cells *in vitro*. The expression of LINC01960-201 in the experimental group was significantly downregulated after LINC01960-201-knockdown (P<0.01), demonstrating that LINC01960-201 was successfully knocked down (Fig. 10A).

The results of RT-qPCR demonstrated that the expression of hsa-miR-608 in the experimental group was significantly

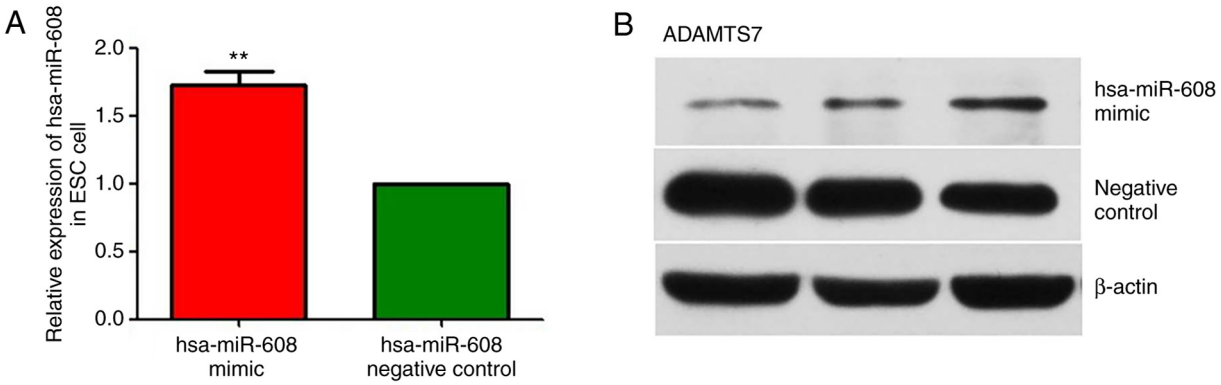

Figure 11. Expression of ADAMTS7 is downregulated after hsa-miR-608 mimic transfection. (A) Changes in the expression of the hsa-miR-608 between the two groups after hsa-miR-608 mimic transfection. (B) Western blotting results of ADAMTS7 expression after hsa-miR-608 mimic transfection between hsa-miR-608 mimic group and negative control. β-actin was used to standardize the data. **P<0.01 vs. negative control. miR, microRNA; ADAMTS7, a disintegrin and metalloproteinase with thrombospondin motifs 7.

higher compared with that in the NC group (P<0.01; Fig. 10B). After devaluation of LINC01960-201 dependence in the endometrial stromal cells, hsa-miR-608 expression was moderately rebounded (Fig. 10B), which demonstrated that there was a mutual regulatory association between LINC01960-201 and hsa-miR-608 in the process of induction of decidualization of endometrial stroma cells *in vitro*. Overall, the expression of hsa-miR-608 was upregulated after LINC01960-201-knockdown.

Effects of hsa-miR-608 mimic transfection during in vitro decidualization. As presented in Fig. 11A, compared with that of the NC group, the expression level of hsa-miR-608 in the experimental group was significantly upregulated (P<0.01), indicating that hsa-miR-608 mimic transfection was successful. Subsequently, the relative protein expression changes of ADAMTS7 were detected by western blotting using β-actin as an internal reference. As presented in Fig. 11B, the strip color detected in the hsa-miR-608 group was markedly lighter compared with that of the NC group (Fig. 11B). With the upregulation of miR-608 expression, the expression of ADAMTS7 in the hsa-miR-608 mimic group was reduced, suggesting that miR-608 has a reverse regulatory effect on ADAMTS7. Overall, the expression of ADAMTS7 was downregulated after hsa-miR-608 mimic transfection during *in vitro* decidualization.

Discussion

The present study used bioinformatics software (miRanda, PITA and RNAhybrid) to demonstrate that hsa-miR-760 and hsa-miR-608 share a common target gene, ADAMTS7, with LINC01960-201. Upon dual luciferase vector construction, plasmid extraction and relative fluorescence value detection, it was revealed that there might be regulatory targets between hsa-miR-608 and the 3'-UTR of ADAMTS7, while there was almost no possibility of regulatory sites between hsa-miR-608 and LINC01960-201, hsa-miR-760 and LINC01960-201 or hsa-miR-760 and the 3'-UTR of ADAMTS7.

In the present study, five samples of endometrial tissues were collected from women suffering from infertility due to endometriosis who underwent laparoscopic surgery. Once the endometrial stromal cells had been extracted for primary cell culture, *in vitro* decidualization was performed with LINC01960-201-knockdown and hsa-miR-608 mimic transfection. RT-qPCR confirmed that LINC01960-201-knockdown was successful. It was revealed that the expression of hsa-miR-608 in the LINC01960-201-knockdown group was increased compared with that of the NC group. After transfection with hsa-miR-608 mimic, RT-qPCR demonstrated that hsa-miR-608 mimic was successfully transfected. Subsequently, the results of western blotting revealed that the band of the hsa-miR-608 mimic transfection group was significantly lighter compared with that of the NC group. With the increase in hsa-miR-608 expression, the expression of ADAMTS7 was decreased, suggesting that hsa-miR-608 has a reverse regulatory effect on ADAMTS7.

The present study also demonstrated that downregulation of LINC01960-201 increased the expression of hsa-miR-608 *in vitro* after induction of decidualization of endometrial stromal cells in women with endometriosis during the period of implantation; while no significant regulatory points were revealed between them in the target verification experiment. hsa-miR-608 expression increased while ADAMTS7 expression decreased, and the target verification experiment revealed that there was a target between the two. The present study indicated that LINC01960-201 played a notable regulatory role in decidualization of the endometrial stromal cells *in vitro* induction in endometriosis, and the expression of LINC01960-201 could not be separated from the regulation of hsa-miR-608 and its ADAMTS7. Therefore, it was hypothesized that the LINC01960-201/hsa-miR-608/ADAMTS7 regulatory pathway plays an important role upon the decidualization of endometrial stromal cells in endometriosis (Fig. 12).

The decidualization does not depend on pregnancy, but can exist independently in humans, and changes in the morphology and activity of endometrial stromal cells via the biological behavior of estrogen and progesterone secreted by the ovaries (1). Decidualization is the process of morphological and biochemical differentiation of endometrial stromal cells into decidual cells (28). Decidualization of endometrial stromal cells is a pivotal element in embryo implantation and

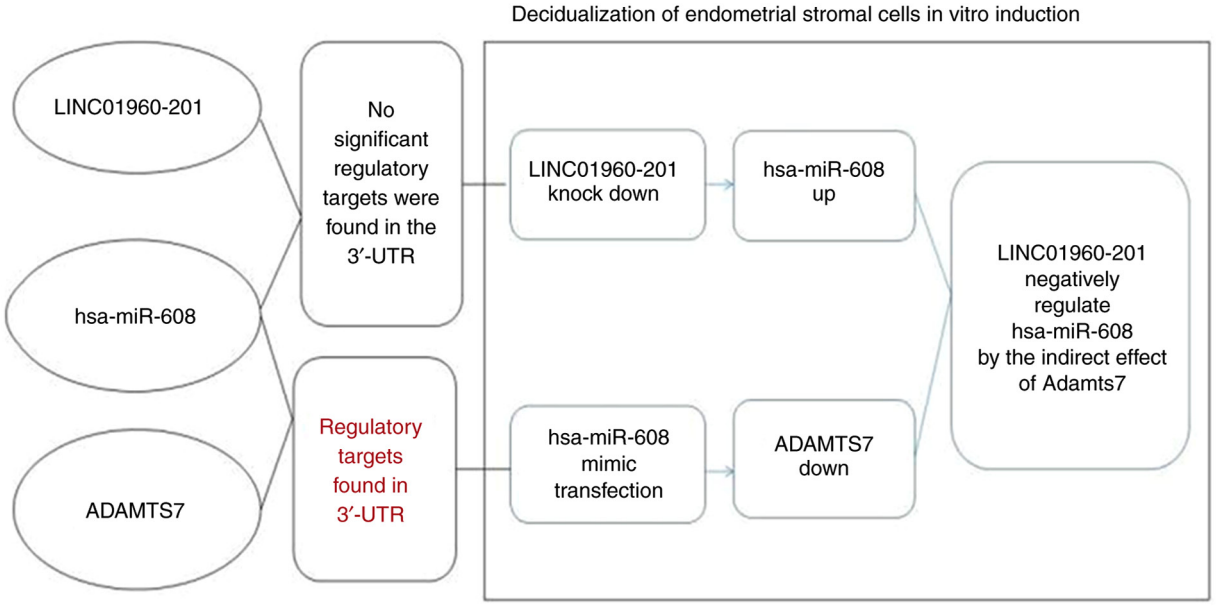

Figure 12. Conclusions of the present study: It was hypothesized that LINC01960-201 may negatively regulate hsa-miR-608 by the indirect effect of ADAMTS7 in the decidualization of endometrial stromal cells in endometriosis.

pregnancy maintenance (29). It has been demonstrated at the transcriptional and protein level that it is a complex gene regulatory network (30,31); however, the regulatory process at the post-transcriptional level is unclear thus far.

Both miRNAs and lncRNAs are non-coding RNAs that play a regulatory role in growth and development, and their common characteristics are to perform their biological functions by the action of mRNA. However, they also have mutual regulatory effects in each other (5,8,32-35). miRNAs can be negatively regulated by lncRNAs in a mechanism similar to that of mRNAs (36). lncRNAs can also be positively regulated by other epigenetic pathways. There are three main mechanisms by which lncRNAs regulate miRNAs (37,38). First, lncRNAs can competitively bind the 3'-UTR of their target gene mRNA to inhibit the negative regulatory mechanism of miRNAs (of note, this signaling pathway is similar to the one described in the present study). The study by Pang *et al* (39) also indicated that lncRNA (by the antisense RNA of BACE1) could be transcribed from the β-secretase-encoded gene locus. This antisense RNA can be complementary to the mRNA of the BACE1 gene and competitively prevent the degradation of miRNA on the BACE1 gene. Secondly, certain lncRNAs can form the precursors of miRNAs through intracellular shear action, thereby processing and producing specific miRNAs, and regulating the expression and function of target genes. Third, certain lncRNAs can act as endogenous miRNA sponges, which in turn can inhibit miRNA expression. Such biological functions indirectly affect the malignant invasion behavior of tumor cells (40). The association between lncRNA ZEB1-AS1 and miR-101/ZEB1 is involved in the proliferation and migration of colon cancer cells (41). The expression of H19 lncRNA and that of integrin β3 in the endometrium of patients with recurrent miscarriages was reduced (42). lncRNA LINC00261 prevents cell proliferation and migration in endometrial stromal cells in patients with endometriosis (17), while lncRNA HOXD cluster antisense RNA 1 promotes the proliferation, migration and invasion of ovarian cancer cells by binding to the miR-608/frizzled family receptor-4 (43).

lncRNAs and miRNAs play an important role in the development of diseases in the female reproductive system. A previous study has stated that exosomal lncRNA CHL1-AS1 derived from peritoneal macrophage can promote the proliferation, invasion and migration of ectopic endometrial stromal cells and inhibit their apoptosis by downregulating miR-610 and upregulating MDM2, which may be a potential target for the treatment of endometriosis (44). Hou *et al* have shown that lncRNA TMPO-AS1 is located in the nucleus and cytoplasm of granulosa-like tumor cells in follicular fluid of women with polycystic ovary syndrome (PCOS), which is likely to inhibit the maturation of miR-335-5p, thereby resulting in PCOS (45). A study of inter-modulation among lncRNA, miRNA and mRNA in estrogen receptor (ER)-positive breast cancer tissues revealed that LINC0092, hsa-miR-449a and hsa-miR-452-5p regulates the co-expression of mRNAs (secreted frizzled-related protein 1 and repulsive guidance molecule A) at the open reading frame (C2orf71) of chromosome 2. This orf contains a 14-node ER-related subtype of the lncRNA-miRNA-mRNA network. It was speculated that LINC0092 and C2orf71 could be used as prognostic indicators for breast cancer (46). Zhou *et al* reported that lncRNA urothelial cancer-associated 1 elevates the expression of HOXA9 by competitively binding with miR-184 in cardiac muscle cells of patients with hypertrophic heart disease, which results in the development and progression of the disease (47). Wambecke *et al* have demonstrated that lncRNA 'UCA1' regulates ovarian cancer response to chemotherapy by binding directly to miR-27a-5p and controlling UBE2N level (48). It was also reported that lncRNA brain cytoplasmic RNA 1 promotes the proliferation, metastasis and invasion of cervical cancer cells (SiHa, HeLa and CaSki) by preventing the expression of miR-138, which is regulated by metalloproteinase-2 (49).

ADAMTS7 is a member of the ADAMTS family, which comprises the family of disintegrin and metalloproteinase associated with thrombospondin motifs. It was reported in aprevious study that this gene plays a main biological role in coronary heart disease (50). Multiple studies have confirmed the regulatory association between lncRNAs, miRNAs and the ADAMTS family (51,52). Dou *et al* have reported that lncRNA HOX transcript antisense RNA promotes the expression of ADAMTS5 in human osteoarthritis chondrocytes by improving the stability of ADAMTS5 mRNA (53). It was hypothesized that the upregulation of ADAMTS7 affects vascular calcification by inhibiting the expression of miR-29a/b, and predicted that this conduction pathway can be possibly used to reduce the incidence and mortality of cardiovascular diseases (54). Hanin *et al* reported that miR-608 is controlled by acetylcholinesterase (AChE) during the occurrence and development of hypertension. Moreover, the expression level of AChE is suppressed due to the interaction between the single nucleotide polymorphism of AChE allele rs17228616 in the 3'-UTR region and miR-608 (55). At the cellular level, attenuating the restraining effects of miR-608 on its negatively regulated cell division control protein 42 homolog and interleukin-6, thus affecting the anxiety of the individual and increasing the risk of hypertension (55).

In our previous studies, abnormal changes were observed in the miRNA, lncRNA and mRNA expression profiles of rats with endometriosis during the implantation window period (22,56). Alignment of the abnormally expressed rat lncRNA sequence with human lncRNA revealed that the similarity between rat lncRNA gi|672045999 |ref|XR_591544.1| and human lncRNA p10107 (LINC01960-201) was estimated to be 83.29% (22). Therefore, LINC01960-201 was selected as the target gene in the present study. The difference between the current study results and the expected ones was that there were no regulatory sites among between hsa-miR-760, LINC01960-201 and ADAMTS7. A limitation of the present study is that the regulatory association between them in the process of decidualization of endometrial stroma cells induced *in vitro* was not further verified. Moreover, the expression of hsa-miR-760 should be further verified. In addition, the expression of ADAMTS7 should be measured after LINC01960-201-knockdown in order to clearly demonstrate the association between the LINC01960-201 and ADAMTS7. Our future studies intend to explore the regulatory role of LINC01960-201 in the decidualization of endometrial stromal cells in the implantation window of healthy women.

Acknowledgements

The authors would like to thank Professor Shan Deng (Department of Obstetrics and Gynecology, Peking Union Medical College Hospital, Peking Union Medical College and Chinese Academy of Medical Sciences, Beijing, China) for their help with sample collection.

Funding

No funding was received.

Availability of data and materials

All data generated or analyzed during this study are included in this published article.

Authors' contributions

JL designed the study. HC designed the study, performed all experiments and analysis, and wrote the paper. HC and JL confirm the authenticity of all the raw data. Both authors have read and approved the final manuscript.

Ethics approval and consent to participate

The present study was approved by the Ethics Committees of Peking Union Medical College Hospital and the Chinese Academy of Medical Sciences (Beijing, China; approval no. S-k332). Written informed consent was obtained from the five patients and all the specimens were acquired with the knowledge of the patients.

Patient consent for publication

Not applicable.

Competing interests

The authors declare that they have no competing interests.

References

1. Minici F, Tiberi F, Tropea A, Orlando M, Gangale MF, Romani F, Campo S, Bompiani A, Lanzone A and Apa R: Endometriosis and human infertility: A new investigation into the role of eutopic endometrium. Hum Reprod 23: 530-537, 2008.
2. Gellersen B, Brosens IA and Brosens JJ: Decidualization of the human endometrium: Mechanisms, functions, and clinical perspectives. Semin Reprod Med 25: 445-453, 2007.
3. He D, Zeng H, Chen J, Xiao L, Zhao Y and Liu N: H19 regulates trophoblastic spheroid adhesion by competitively binding to let-7. Reproduction 157: 423-430, 2019.
4. Staun-Ram E and Shalev E: Human trophoblast function during the implantation process. Reprod Biol Endocrinol 3: 56, 2005.
5. Hansen TB, Wiklund ED, Bramsen JB, Villadsen SB, Statham AL, Clark SJ and Kjems J: miRNA-dependent gene silencing involving Ago2-mediated cleavage of a circular antisense RNA. EMBO J 30: 4414-4422, 2011.
6. Gellersen B and Brosens JJ: Cyclic decidualization of the human endometrium in reproductive health and failure. Endocr Rev 35: 851-905, 2014.
7. Lessey BA, Castelbaum AJ, Buck CA, Lei Y, Yowell CW and Sun J: Further characterization of endometrial integrins during the menstrual cycle and in pregnancy. Fertil Steril 62: 497-506, 1994.
8. Barragan F, Irwin JC, Balayan S, Erikson DW, Chen JC, Houshdaran S, Piltonen TT, Spitzer TLB, George A, Rabban JT, *et al*: Human endometrial fibroblasts derived from mesenchymal progenitors inherit progesterone resistance and acquire an inflammatory phenotype in the endometrial niche in endometriosis. Biol Reprod 94: 118, 2016.
9. Takano M, Lu Z, Goto T, Fusi L, Higham J, Francis J, Withey A, Hardt J, Cloke B, Stavropoulou AV, *et al*: Transcriptional cross talk between the forkhead transcription factor forkhead box O1A and the progesterone receptor coordinates cell cycle regulation and differentiation in human endometrial stromal cells. Mol Endocrinol 21: 2334-2349, 2007.
10. Lessey BA and Kim JJ: Endometrial receptivity in the eutopic endometrium of women with endometriosis: It is affected, and let me show you why. Fertil Steril 108: 19-27, 2017.

11. Atkins HM, Lombardini ED, Caudell DL, Appt SE, Dubois A and Cline JM: Decidualization of endometriosis in macaques. Vet Pathol 53: 1252-1258, 2016.
12. Petracco R, Dias ACO, Taylor H, Petracco A, Badalotti M, Da Rosa Michelon J, Marinowic DR, Hentschke M, De Azevedo PN, Zanirati G and Machado DC: Evaluation of miR-135a/b expression in endometriosis lesions. Biomed Rep 11: 181-187, 2019.
13. Ghazal S, McKinnon B, Zhou J, Mueller M, Men Y, Yang L, Mueller M, Flannery C, Huang Y and Taylor HS: H19 lncRNA alters stromal cell growth via IGF signaling in the endometrium of women with endometriosis. EMBO Mol Med 7: 996-1003, 2015.
14. Liu S, Qiu J, Tang X, Cui H, Zhang Q and Yang Q: lncRNA-H19 regulates cell proliferation and invasion of ectopic endometrium by targeting ITGB3 via modulating miR-124-3p. Exp Cell Res 381: 215-222, 2019.
15. Li K, Wu Y, Yang H, Hong P, Fang X and Hu Y: H19/miR-30a/C8orf4 axis modulates the adipogenic differentiation process in human adipose tissue-derived mesenchymal stem cells. J Cell Physiol 234: 20925-20934, 2019.
16. Liang Z, Chen Y, Zhao Y, Xu C, Zhang A, Zhang Q, Wang D, He J, Hua W and Duan P: miR-200c suppresses endometriosis by targeting MALAT1 in vitro and in vivo. Stem Cell Res Ther 8: 251, 2017.
17. Sha L, Huang L, Luo X, Bao J, Gao L, Pan Q, Guo M, Zheng F and Wang H: Long non-coding RNA LINC00261 inhibits cell growth and migration in endometriosis. J Obstet Gynaecol Res 43: 1563-1569, 2017.
18. Wang H, Shi G, Li M, Fan H, Ma H and Sheng L: Correlation of IL-1 and HB-EGF with endometrial receptivity. Exp Ther Med 16: 5130-5136, 2018.
19. Cai QF, Wan F, Dong XY, Liao XH, Zheng J, Wang R, Wang L, Ji LC and Zhang HW: Fertility clinicians and infertile patients in China have different preferences in fertility care. Hum Reprod 29: 712-719, 2014.
20. Grechukhina O, Petracco R, Popkhadze S, Massasa E, Paranjape T, Chan E, Flores I, Weidhaas JB and Taylor HS: A polymorphism in a let-7 microRNA binding site of KRAS in women with endometriosis. EMBO Mol Med 4: 206-217, 2012.
21. Meuleman C, Vandenabeele B, Fieuws S, Spiessens C, Timmerman D and D'Hooghe T: High prevalence of endometriosis in infertile women with normal ovulation and normospermic partners. Fertil Steril 92: 68-74, 2009.
22. Cai H, Zhu X, Li Z, Zhu Y and Lang J: lncRNA/mRNA profiling of endometriosis rat uterine tissues during the implantation window. Int J Mol Med 44: 2145-2160, 2019.
23. Crossley BM, Bai J, Glaser A, Maes R, Porter E, Killian ML, Clement T and Toohey-Kurth K: Guidelines for sanger sequencing and molecular assay monitoring. J Vet Diagn Invest 32: 767-775, 2020.
24. Shen L, Hu P, Zhang Y, Ji Z, Shan X, Ni L, Ning N, Wang J, Tian H, Shui G, *et al*: Serine metabolism antagonizes antiviral innate immunity by preventing ATP6V0d2-mediated YAP lysosomal degradation. Cell Metab 33: 971-987.e6, 2021.
25. Lv H, Lv G, Chen C, Zong Q, Jiang G, Ye D, Cui X, He Y, Xiang W, Han Q, *et al*: NAD (+) metabolism maintains inducible PD-L1 expression to drive tumor immune evasion. Cell Metab 33: 110-127.e5, 2021.
26. Roux P, Perrin J, Mancini J, Agostini A, Boubli L and Courbiere B: Factors associated with a poor prognosis for the IVF-ICSI live birth rate in women with rAFS stage III and IV endometriosis. J Assist Reprod Genet 34: 921-928, 2017.
27. Livak KJ and Schmittgen TD: Analysis of relative gene expression data using real-time quantitative PCR and the 2 (-Delta Delta C (T)) method. Methods 25: 402-408, 2001.
28. Szwarc MM, Hai L, Gibbons WE, Peavey MC, White LD, Mo Q, Lonard DM, Kommagani R, Lanz RB, DeMayo FJ and Lydon JP: Human endometrial stromal cell decidualization requires transcriptional reprogramming by PLZF. Biol Reprod 98: 15-27, 2018.
29. Rytkonen KT, Erkenbrack EM, Poutanen M, Elo LL, Pavlicev M and Wagner GP: Decidualization of human endometrial stromal fibroblasts is a multiphasic process involving distinct transcriptional programs. Reprod Sci 26: 323-336, 2019.
30. Vasquez YM, Mazur EC, Li X, Kommagani R, Jiang L, Chen R, Lanz RB, Kovanci E, Gibbons WE and DeMayo FJ: FOXO1 is required for binding of PR on IRF4, novel transcriptional regulator of endometrial stromal decidualization. Mol Endocrinol 29: 421-433, 2015.
31. Feng C, Shen JM, Lv PP, Jin M, Wang LQ, Rao JP and Feng L: Construction of implantation failure related lncRNA-mRNA network and identification of lncRNA biomarkers for predicting endometrial receptivity. Int J Biol Sci 14: 1361-1377, 2018.
32. Cazalla D, Yario T and Steitz JA: Down-regulation of a host microRNA by a herpesvirus saimiriNoncoding RNA. Science 328: 1563-1566, 2010.
33. Guttman M, Donaghey J, Carey BW, Garber M, Grenier JK, Munson G, Young G, Lucas AB, Ach R, Bruhn L, *et al*: lincRNAs act in the circuitry controlling pluripotency and differentiation. Nature 477: 295-300, 2011.
34. Hansen TB, Jensen TI, Clausen BH, Bramsen JB, Finsen B, Damgaard CK and Kjems J: Natural RNA circles function as efficient microRNA sponges. Nature 495: 384-388, 2013.
35. Braza-Boils A, Mari-Alexandre J, Gilabert J, Sánchez-Izquierdo D, España F, Estellés A and Gilabert-Estellés J: MicroRNA expression profile in endometriosis: Its relation to angiogenesis and fibrinolytic factors. Hum Reprod 29: 978-988, 2014.
36. Xu JH, Chang WH, Fu HW, Yuan T and Chen P: The mRNA, miRNA and lncRNA networks in hepatocellular carcinoma: An integrative transcriptomic analysis from gene expression omnibus. Mol Med Rep 17: 6472-6482, 2018.
37. Song X, Cheng L, Zhou T, Guo X, Zhang X, Chen YPP, Han P and Sha J: Predicting miRNA-mediated gene silencing mode based on miRNA-target duplex features. Comput Biol Med 42: 1-7, 2012.
38. Li F, Orban R and Baker B: SoMART: A web server for plant miRNA, tasiRNA and target gene analysis. Plant J 70: 891-901, 2012.
39. Pang M, Xing C, Adams N, Rodriguez-Uribe L, Hughs SE, Hanson SF and Zhang J: Comparative expression of miRNA genes and miRNA-based AFLP marker analysis in cultivated tetraploid cottons. J Plant Physiol 168: 824-830, 2011.
40. Brodersen P, Sakvarelidze-Achard L, Schaller H, Khafif M, Schott G, Bendahmane A and Voinnet O: Isoprenoid biosynthesis is required for miRNA function and affects membrane association of ARGONAUTE 1 in *Arabidopsis*. Proc Natl Acad Sci USA 109: 1778-1783, 2012.
41. Xiong WC, Han N, Wu N, Zhao KL, Han C, Wang HX, Ping GF, Zheng PF, Feng H, Qin L and He P: Interplay between long noncoding RNA ZEB1-AS1 and miR-101/ZEB1 axis regulates proliferation and migration of colorectal cancer cells. Am J Transl Rese 10: 605-617, 2018.
42. Zeng H, Fan X and Liu N: Expression of H19 imprinted gene in patients with repeated implantation failure during the window of implantation. Arch Gynecol Obstet 296: 835-839, 2017.
43. Wang Y, Zhang W, Wang Y and Wang S: HOXD-AS1 promotes cell proliferation, migration and invasion through miR-608/FZD4 axis in ovarian cancer. Am J Cancer Res 8: 170-182, 2018.
44. Liu T, Liu M, Zheng C, Zhang D, Li M and Zhang L: Exosomal lncRNA CHL1-AS1 derived from peritoneal macrophages promotes the progression of endometriosis via the miR-610/MDM2 Axis. Int J Nanomedicine 16: 5451-5464, 2021.
45. Hou F, Li J, Peng J, Teng Z, Feng J and Xia W: lncRNA TMPO-AS1 suppresses the maturation of miR-335-5p to participate in polycystic ovary syndrome. J Ovarian Res 14: 99, 2021.
46. Xiao B, Zhang W, Chen L, Hang J, Wang L, Zhang R, Liao Y, Chen J, Ma Q, Sun Z and Li L: Analysis of the miRNA-mRNA-lncRNA network in human estrogen receptor-positive and estrogen receptor-negative breast cancer based on TCGA data. Gene 658: 28-35, 2018.
47. Zhou G, Li C, Feng J, Zhang J and Fang Y: lncRNA UCA1 is a novel regulator in cardiomyocyte hypertrophy through targeting the miR-184/HOXA9 axis. Cardiorenal Med 8: 130-139, 2018.
48. Wambecke A, Ahmad M, Morice PM, Lambert B, Weiswald LB, Vernon M, Vigneron N, Abeilard E, Brotin E, Figeac M, *et al*: The lncRNA 'UCA1' modulates the response to chemotherapy of ovarian cancer through direct binding to miR-27a-5p and control of UBE2N levels. Mol Oncol 15: 3659-3678, 2021.
49. Peng J, Hou F, Feng J, Xu SX and Meng XY: Long non-coding RNA BCYRN1 promotes the proliferation and metastasis of cervical cancer via targeting microRNA-138 *in vitro* and *in vivo*. Oncol Lett 15: 5809-5818, 2018.
50. Mizoguchi T, MacDonald BT, Bhandary B, Popp NR, Laprise D, Arduini A, Lai D, Zhu QM, Xing Y, Kaushik VK, *et al*: Coronary disease association with ADAMTS7 is due to protease activity. Circ Res 129: 458-470, 2021.

51. Yao N, Peng S, Wu H, Liu W, Cai D and Huang D: Long noncoding RNA PVT1 promotes chondrocyte extracellular matrix degradation by acting as a sponge for miR-140 in IL-1β-stimulated chondrocytes. J Orthop Surg Res 17: 218, 2022.
52. Zhang X, Li D, Jia C, Cai H, Lv Z and Wu B: METTL14 promotes tumorigenesis by regulating lncRNA OIP5-AS1/miR-98/ADAMTS8 signaling in papillary thyroid cancer. Cell Death Dis 12: 617, 2021.
53. Dou P, Hu R, Zhu W, Tang Q, Li D, Li H and Wang W: Long non-coding RNA HOTAIR promotes expression of ADAMTS-5 in human osteoarthritic articular chondrocytes. Pharmazie 72: 113-117, 2017.
54. Du Y, Gao C, Liu Z, Wang L, Liu B, He F, Zhang T, Wang Y, Wang X, Xu M, *et al*: Upregulation of a disintegrin and metalloproteinase with thrombospondin motifs-7 by miR-29 repression mediates vascular smooth muscle calcification. Arterioscler Thromb Vasc Biol 32: 2580-2588, 2012.
55. Hanin G, Shenhar-Tsarfaty S, Yayon N, Yau YH, Bennett ER, Sklan EH, Rao DC, Rankinen T, Bouchard C, Geifman-Shochat S, *et al*: Competing targets of microRNA-608 affect anxiety and hypertension. Hum Mol Genet 23: 4569-4580, 2014.
56. Cai H, Zhu XX, Li ZF and Lang JH: MicroRNA dysregulation and steroid hormone receptor expression in uterine tissues of rats with endometriosis during the implantation window. Chin Med J (Engl) 131: 2193-2204, 2018.